STRUCTURE SAFETY AND WELD STRENGTH EVALUATION BY METALLIC WELD JOINTS IN FCAW WITH TAGUCHI DESIGN

M. Saravanan, G. Mutharasu, Sangeetha Krishnamoorthi, M. Saravanakumar and B. Selvababu
Aarupadai Veedu Institute of Technology, Vinayaka Mission's Research Foundation, Deemed to be University, Tamil Nadu, India
E-Mail: saravanan2103m@gmail.com

ABSTRACT

Several industries, including shipbuilding and automobile manufacturing, extensively use welding as a joining method. Welding processes are always plagued by distortion. Many parameters influence distortion on weld joints, including the properties of materials and welding parameters. To obtain optimal distortion parameters, the Shielded Metal Arc Welding (SMAW) process on angular distortion is used. However, this technique contains slag inclusions and it gives low productivity. To overcome this issue the Flux-Cored Arc Welding (FCAW) technique is used to combine the metals and alloys in a variety of sectors. It offers several advantages over other methods, including simplicity and adaptability over Submerged-arc welding (SAW), higher productivity over SMAW, and superior surface appearance. In this work, during the welding operation, two dissimilar high-carbon steels (EN8 and EN19) are used and the welding quality is checked by utilizing destructive and microstructure tests. To analyze the effects of process parameters on welded joints, mechanical tests like yield strength, tensile strength, and hardness test are performed and optimized using TAGUCHI design (L9 array). The accurate input parameter of EN8 and EN19 steel with a thickness of 6mm is determined. The welding process parameters are optimized by utilizing the MINITAB-17 software. As a result, the FCAW has higher tensile and yield strength than the conventional method of SAW.

Keywords: flux-cored Arc welding EN8, shielded metal Arc welding and EN19 steel, destructive and microstructure tests, TAGUCHI design (L9 array), MINITAB-17 software.

Manuscript Received 28 July 2023; Revised 6 December 2023; Published 10 January 2024

1. INTRODUCTION

Steel is a crucial structural element that is used in many industries, including building, the marine sector, and the automotive industry. Materials corrosion causes significant financial losses. Corrosion mostly contributes to the destruction of the metal by its response to the exposed media [1-2]. One of the most important and common industrial methods utilised with these alloys is welding. In machinery and the construction of buildings, Welding has played a significant role [3]. Robotic gas metal arc (GMA) welding is a production method for creating high-quality joints that also be applied to automation systems to increase productivity. Despite being widely used across many manufacturing sectors, a thorough understanding and quantification of the mathematical models for the process strictures for specific welding operations are required to completely automate robotic GMA welding [4]. The previous study evaluated laser welding for the combinations of dissimilar materials without the filler metal. However, it is important to address mechanical qualities and welding zone flaws and the filler metal prevents high-manganese steel from being maximised or from having good mechanical qualities [5]. The best method of welding for joining materials that are significantly different from one another, such as ceramic to glass, glass to metal, and others, which is diffusion welding. In contrast to fusion welding, this method of welding has several important drawbacks, including complicated equipment, low productivity and a limited range of work piece sizes, etc [7]. FSW has become a viable substitute for conventional fusion welding methods. In this solid-state joining process, facing surfaces as well as the joining line are inserted into the work piece and a spinning tool is introduced to create a complex stirring of the material. Investigation of the factor correlations and their impacts on the total structural rigidity is still required to offer acceptable process control for industrial applications [8-9]. SMAW is manual metal arc welding, which is widely used for producing structural components due to the versatility of the equipment as well as the welding position. But, this method gives low productivity and contains slag inclusions [10-11]. Therefore, the FCAW process is employed in this study, it has several advantages over other processes, including high position rates, greater tolerance for rust as well as mill scale than GMAW, simplicity and adaptability over SAW, less operator expertise needed over GMAW, higher productivity over SMAW and better surface appearance. Numerous elements of microstructures and their influence on the mechanical behavior of metals have been researched. An important area of research is the fabrication of various materials by properly changing their microstructure. In general, the metal develops more resistant to plastic flow (yield strength increases) as the average grain size drops and the opposite effect on strength arises as the grain size increases (yield strength reduces). Some heat treatments can alter the characteristics of steel and enhance corrosion resistance. Metals have their microstructure, corrosion resistance, and mechanical properties changed through heat treatment processes such as normalising, annealing, tempering, and hardening. [12-13].

Non-Destructive Examination (NDE) is a series of analysis procedures that are widely used in the defense

ARPN Journal of Engineering and Applied Sciences

and aerospace industries to assess a material's attributes. NDE is crucial for checking materials for flaws without affecting their physical characteristics [14]. Additionally, investigations on the relationship between bead geometry as well as weldability have been conducted in the past to enhance welding quality by identifying the critical elements influencing bead formation. However, the relevance of investigation and consideration confined to bead geometry in the actual field has been minimized because comparable size areas as well as heat-affected regions are intermittently derived even for diverse welding process factors. As a result, a multi-perspective analysis is required to accurately identify the explicit conditions, which have similar bead geometry to the intermittent variables [15]. Additionally, Alumina forming austenitic (AFA) steel is a modern high-temperature unaffected stainless steel. It offers exceptional high-temperature creep strength as well as corrosion resistance. However, the AFA steel has cost [16-17]. AISI 1040 steel or EN8 steel are examples of non-alloy medium carbon steel [18]. EN8 and EN19 are utilized in this work because they give a better tensile strength than the other steel. The effects of each weld processing stricture have been studied by utilizing the Taguchi model on weld geometries as well as mechanical properties [19-20]. The aforementioned facts, the Taguchi model with L9 orthogonal array as well as ANOVA is utilized in this work.

The proposed work discussed the structure safety and weld strength of the metallic weld joints in FCAW with the Taguchi design method. FCAW technique is used to combine metals and alloys in a variety of sectors and it has higher productivity over SMAW and superior surface appearance. EN8 and EN19 are used and the welding quality is checked by utilizing destructive and microstructure tests. To analyze the effects of process parameters on welded joints, mechanical tests, hardness, and bead geometry analysis are performed and optimized using TAGUCHI design (L9 array). The welding process parameters are optimized by utilizing the MINITAB-17 software. As a result, the accurate input parameter of EN8 and EN19 steel with a thickness of 6mm is determined.

2. EXPERIMENTAL PROCEDURE

The steel grades of medium carbon EN8 and EN19 have been selected in the proposed work. Non-destructive tests, tensile tests, flexural tests, and microstructural analysis are carried out in the testing process. Validation tests for the Hardness test and tensile strength test are carried out by the TAGUCHI method as illustrated in Figure-1.

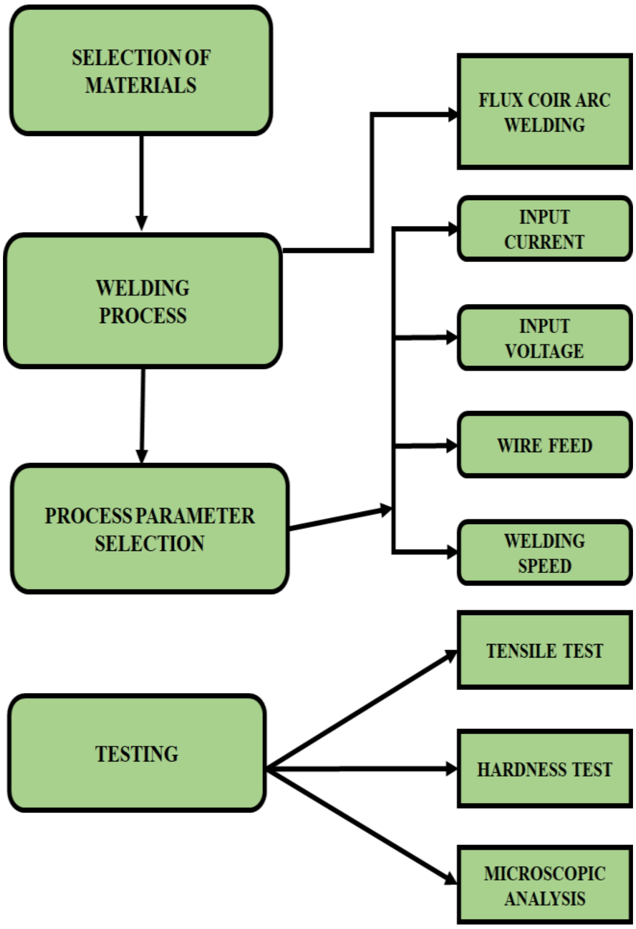

Figure-1. Flowchart for the process of experiment.

A. Material Selection

The steel grades EN8 and EN19 have been selected for this study as specified in Figure-2. The EN8 and EN19 steel is a type of plain carbon steel with 0.40% carbon in its structure, so it is termed as medium carbon steel. Table-1 provides the standard chemical composition of EN8 steel. Also, EN19 steel has a carbon percentage of 0.36 to 0.44%, which has high strength and excellent quality. The qualities of ductility in medium carbon steel are favourable and the chemical composition of EN19 steel alloy is shown in Table-2.

Table-1. Chemical composition of EN 8 Steel.

S. No	ELEMENT	COMPOSITION IN WEIGHT %	
		MIN	MAX
1	Chromium, Cr	0.4	0.6
2	Phosphorus	0.10	0.06
3	Sulphur	-	0.06
4	Manganese	0.6	1.00
5	Carbon, C	0.35	0.45
6	Silicon, Si	0.05	0.35

ARPN Journal of Engineering and Applied Sciences

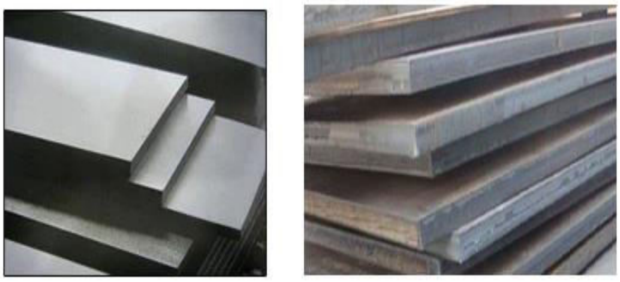

(a) (b)

Figure-2. (a) EN8 and (b) EN19 steel plate.

Table-2. Chemical composition of EN19 steel alloy.

S. No	Chemical composition	Weight
1.	Carbon, C	0.44
2.	Manganese	0.70
3.	Silicon	0.40
4.	Sulphur	0.05
5.	Phosphorus	0.05
6.	Chromium	0.9

B. Welding Process

A weld joint is formed by arranging the edge preparations. The pieces are to be welded and connected, or a gap is used to ensure penetration. Most joint gaps are located at the root of the joint, which is the bottom part of the joint. Root opening or open roots are terms used to describe this condition. For example; an open root V groove. In some cases, a back weld is applied to a joint, if the joint design allows it, the background strip or insert is used to make welding easier.

Figure-3. Open root “V” groove.

C. Experimental Setup

In the experiment, an AC constant current Sun power source (DC Inverter machine MIG 500-IGBT) is employed. Sun Power MIG 500 IGBT machines are employed for this welding work. Setting welding (electrode position, voltage, welding current, wire feed rate, arc travel speed) and connecting the joint in fixtures are necessary steps in the procedure**.** The proper relationship between voltages, current gas flow, welding speed as well as gun angles has been achieved by properly configuring the welding parameters. The right filler wires and shielding gases are chosen. It is important to give attention to arc glares, smokes, fumes, electrode changes and nozzle cleaning during welding. Also, it is necessary to examine the quality of weld bead appearance after the welding is completed.

Figure-4. MIG Welding machine.

Figure-5 depicts the flux cored arc welding schematic diagram. The welding test piece used in the size of 100mm × $100mm \times 6mm$ of EN8 and EN19 steel.

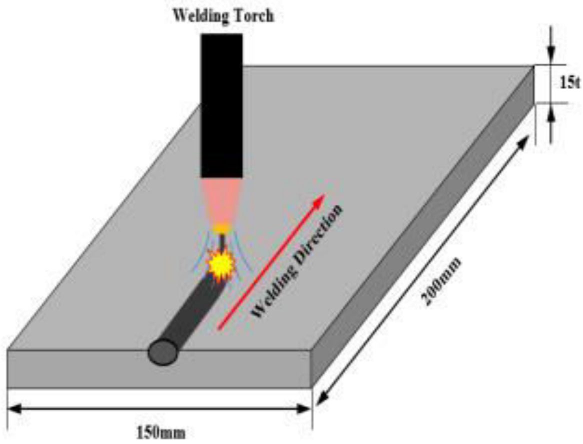

Figure-5. Schematic diagram of FCAW.

D. Non-Destructive Test

A technique for assessing a material without causing destruction is non-destructive testing (NDT). This refers to the examination, and calculation of the welded joints' materials, constituents, or any faults exposed in the welded portion or the distinctions between the materials' properties without causing material damage. Four types of Non-destructive tests are used in this work such as magnetic particle test, Visual inspection, Ultrasonic test, and liquid penetration test.

Visual testing: The most typical method of material inspection is visual testing. It is a method of visually inspecting a piece of material by a qualified

VOL. 18, NO. 21, NOVEMBER 2023 ISSN 1819-6608
ARPN Journal of Engineering and Applied Sciences

inspector while utilising their unaided or aided vision to find problems. The pipelines, pressure vessels, storage tanks, and other welded surfaces, as well as their interior and external surfaces, are all able to be tested visually. It contains low cost when compared to the other techniques.

Magnetic particle testing: The yoke approach is used to test the low carbon weld plates with two different forms of the current, first method is alternating current (AC), which is utilised to identify surface breaks. The second method is Direct current (DC), which is an additional option for locating subsurface discontinuities. By varying the yoke's position in multiple directions, the experiment is performed two to three times.

Liquid penetration test: By allowing a coloured visible as well as a fluorescent dye to flow out from the defective area, liquid penetration testing is used to identify the surface discontinuities. It is a tried and true NDT technique for locating flaws. Cleaner, penetrate and developer are the three materials used in this technique. This technique is inexpensive and it is used to place the surface breaking defects in non-porous materials. All ferrous as well as non-ferrous materials are works under this process. Initially, the testing material is scattered with the penetrant. The designer draws out the penetrant flaws from the surface to an observable indication while the additional penetrant is removed by the remover.

Ultrasonic testing: Ultrasonic testing is carried out in FCAW, based on the rapidity of sound in the material; high frequency waves are presented in the welding process under inspection to identify surface defects as well as internal defects. These waves are reflected at interfaces with some attenuation.

E. Tensile Test

Determine the joints' tensile and yield strengths. The welded samples are made by the ASTM EN8 and EN19 standards. Using standard testing tools, the tensile strength of the welded piece is determined. Wire cut electrical discharge machining is employed to cut the tensile testing sample. T Wire electrical discharge machining (WEDM) employs a thin electrode wire to cut or shape a work item typically made of conductive material along a well-planned path.

Figure-6. Sample for tensile test.

F. Hardness Test

A Rockwell hardness test is conducted to determine the hardness of the specimen using a diamond indenter. According to EN8 and EN19 steel standards, the hardness of steel is measured on the C-scale4, and a diamond indenter is used during the process. Indenter is placed on surface of specimen and minor load is applied to needle at C-0. The crank lever is then moved from position A to position B, and the major load is given for a dwell time to allow the elastic recovery. Once the major load is detached, the depth of indentation is calculated and the hardness value is obtained.

G. Microstructural Analysis

A material's micro structural properties alter dramatically when examined at different length scales. To properly characterize the microstructure of a material, it is essential to take the length scale (100X) of your observations into account. The microstructural analysis is made for 5 samples in FCAW, sample 3 and 5 give the best grain structure than the GMAW.

3. RESULT AND DISCUSSIONS

In this research, the proposed work is compared with the conventional techniques, and the graph is obtained for tensile test, impact test, and hardness test by using EN8 and EN19 steel. To analyze the effects of process parameters on welded joints, mechanical tests like yield strength, tensile strength, and hardness tests are performed. Taguchi Orthogonal array is aimed in minitab-17 to determine the S/N ratio. As a result, the comparison graph obtained for FCAW and SAW, from that the proposed technique achieves higher strength than the conventional methods. The microstructural analysis is made for 5 samples in FCAW, samples 3 and 5 give the best grain structure than the GMAW.

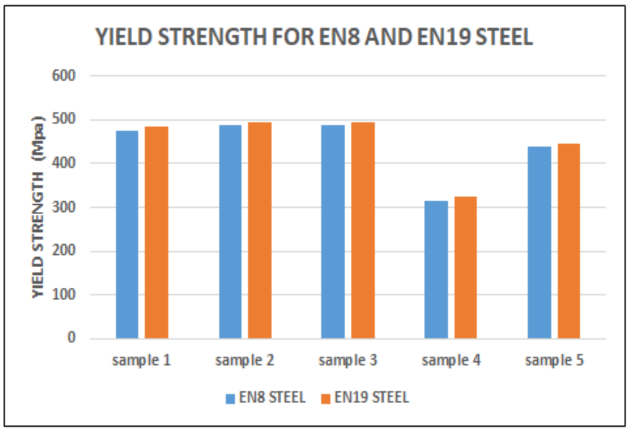

Figure-7. Yield strength for EN8 and EN 19 steel.

The yield strength for EN8 and EN19 steel is represented in Figure-7, it is observed that 5 samples are taken to determine the strength in EN8 and EN19 steel. EN19 attains higher strength than EN8 as well and samples 2 and 3 give high strength than the other samples.

ARPN Journal of Engineering and Applied Sciences

Table-3. Tensile strength of EN8 welded samples.

S. No	Voltage (V)	Current (A)	Welding speed (mm/min)	Wire feed m/min	Tensile strength Mpa	Yield strength Mpa
Sample 1	23.7	196	83	6.5	532.893	475.08
Sample 2	22.8	189	77	5.15	553.120	486.92
Sample 3	21.12	172	75	5.9	560	484.213
Sample 4	21.9	165	72	5.3	518.027	316.307
Sample 5	21.4	159	67	4.9	487.880	439.8

The tensile strength of EN8 welded samples is illustrated in Table-3. the maximum tensile strength (560 MPa) and yield strength (484 MPa) for sample 3, are measured using a predefined experiment with the parameters of voltage 21.12 v, current 170A, Wire feed rate is 5.9 m/min, welding speed is 75mm. The welding strength of sample 3 has increased with an input of average current

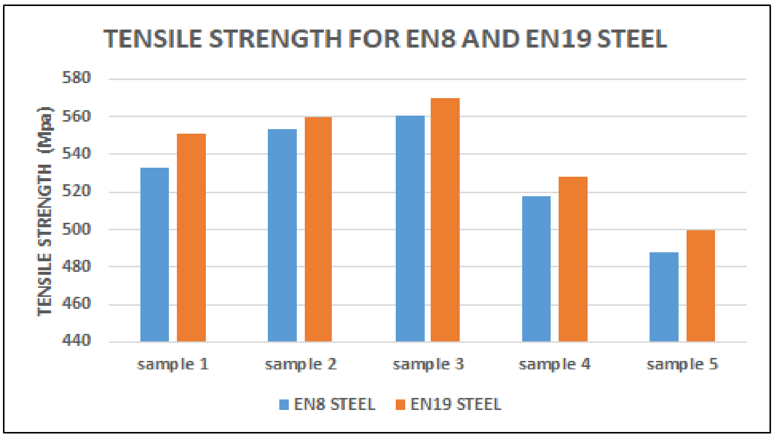

Figure-8. Tensile strength for EN8 and EN19 steel.

Figure-8 represents the tensile strength of EN8 and EN 19 steel, from the figure it is analyzed that 5 samples are taken to calculate the strength of EN8 and EN19. As a result, Samples 2 and 3 have higher strength than the other samples as well and EN19 attains higher strength than the EN8 steel.

Table-4 specifies the tensile strength of EN19 welded samples. The maximum tensile strength for (570 MPa) and yield strength (493MPa) for sample 3, are measured using a predefined experiment with the parameters of voltage 21.12 v, current 172A, Wire feed rate is 5.9 m/min, welding speed is 75mm. The welding strength of sample 3 has increased with an input of average current.

Table-4. Tensile strength of EN19 welded samples.

S. No	Voltage (V)	Current (A)	Welding speed (mm/min)	Wire feed m/min	Tensile strength Mpa	Yield strength Mpa
Sample 1	23.7	196	83	6.5	550.78	485.12
Sample 2	22.8	189	77	5.15	560	495.34
Sample 3	21.12	172	75	5.9	570.34	493.123
Sample 4	21.9	165	72	5.3	528.213	326.12
Sample 5	21.4	159	67	4.9	500	444.93

ARPN Journal of Engineering and Applied Sciences

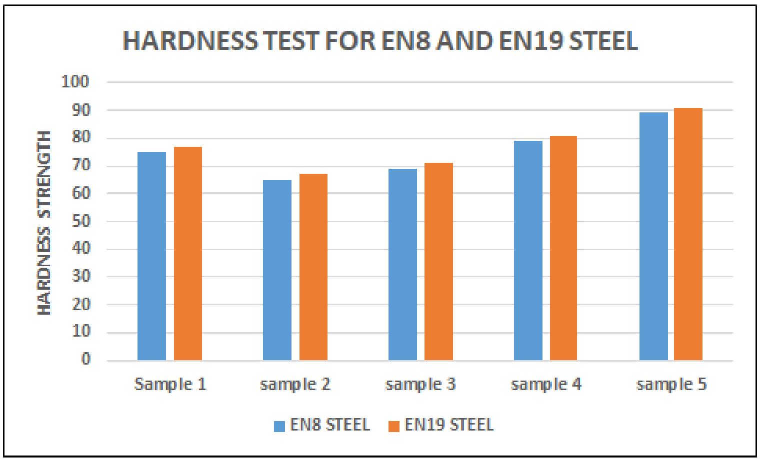

Figure-9. Hardness test for EN8 and EN19 steel.

Hardness test for EN8 and EN19 steel is illustrated in Figure-9, which is analyzed that 5 sample is taken for the test, from the test result sample 3 obtained good hardness than the other sample. Moreover, Compared to EN8, EN19 attains high strength.

Table-5. Rockwell hardness test for EN8 and EN19 steel.

S.No	Voltage (V)	Current (A)	Welding speed (mm/min)	Wire feed m/min	Rockwell hardness test	
					EN8 steel	EN19 steel
Sample 1	24	192	82	6.3	75	77
Sample 2	23.5	181	77	5.9	65	67
Sample 3	22.1	172	72	5.7	69	71
Sample 4	22.07	163	67	5.3	79	81
Sample 5	22.01	152	63	4.9	89	91

Table-5 presents the results from an evaluation of hardness in welded samples for EN8 and EN19 steel. Sample 5 shows the highest hardness value of 89 and 91N/mm^2, according to a predefined experiment, which has a welding speed is 63 mm/min, wire feed is 4.9 m/min, voltage is 22.01 volts, current is 152 amps as specified in above table.

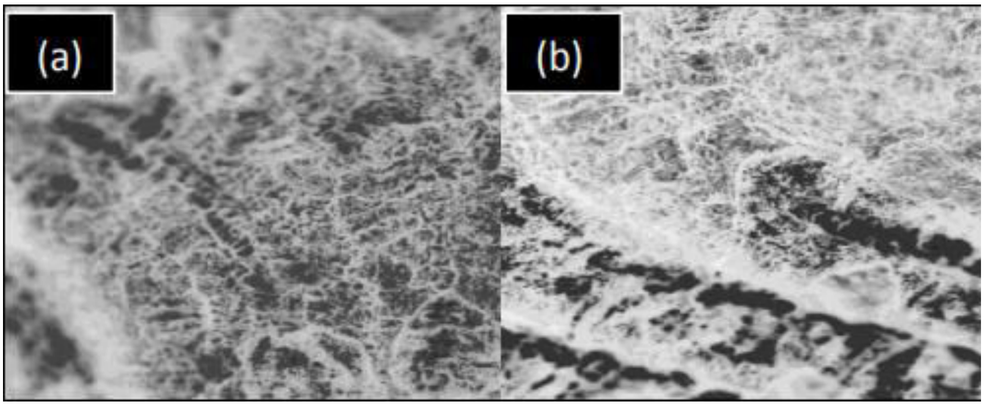

Figure-10. Microstructure analysis for (a) sample 3 and (b) sample 5.

The five samples are studied distinctly in FCAW-welded sample areas and the microstructure of the intended area is identified by examining the microstructure of the samples. Samples 3 and 5's visual results are shown in Figure-10. For grain structure, samples 3 and 5 exhibited the best microstructure.

ISSN 1819-6608
ARPN Journal of Engineering and Applied Sciences

Table-6. Factor distribution and experimental layout of Orthogonal array (L_9).

No.	Factors			
	Electrode	Current (A)	Voltage (V)	speed
1	E308	140	14	4
2	E308	140	16	5
3	E308	140	18	6
4	E309	160	16	6
5	E309	160	18	4
6	E309	160	14	5
7	E312	180	18	5
8	E312	180	14	6
9	E312	180	16	4

Table-6 represents the orthogonal arrays (L9) experimental design and factor distribution. Which contains the electrode, different factors like current; voltage, and speed with different variables are specified in the above table.

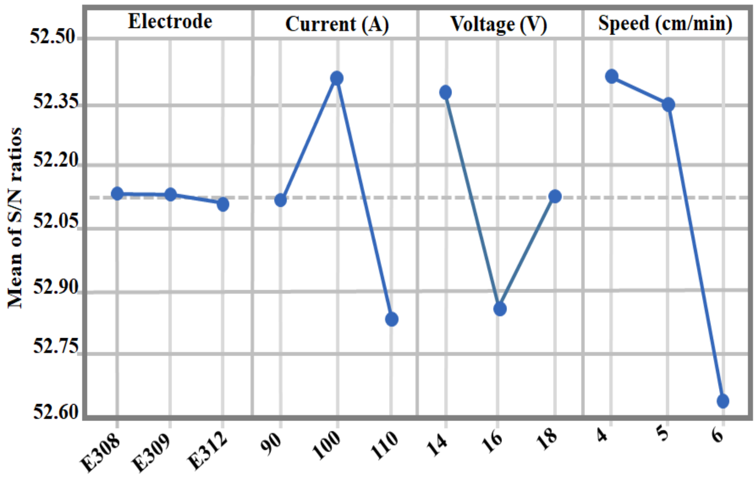

Figure-11. Hardness against various factors.

Figure-11 demonstrates the importance of welding current and electrode type when assessing the increase in hardness. The minimal hardness is achieved at 16 volts of arc voltage as the welding speed increases.

ARPN Journal of Engineering and Applied Sciences

www.arpnjournals.com

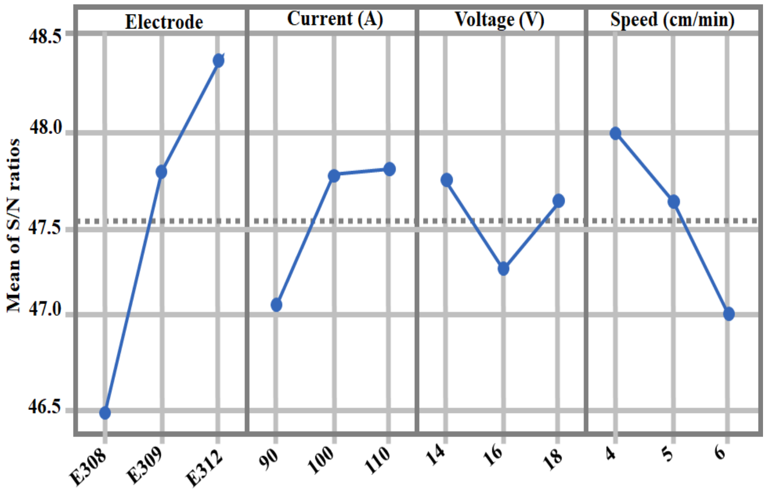

Figure-12. Tensile strength against various factors.

Figure-12 displays a study of tensile strength's signal-to-noise (S/N) ratio. An electrode type of E 308, a welding current of 100A, an arc voltage of 14 V as well a welding speed of 4 cm/min provide the largest yield of tensile strength S/N ratio.

Figure-13 represents the Taguchi method, which gives the result of a hardness strength of 410 (N/mm^2) and tensile strength of 550 (Mpa)

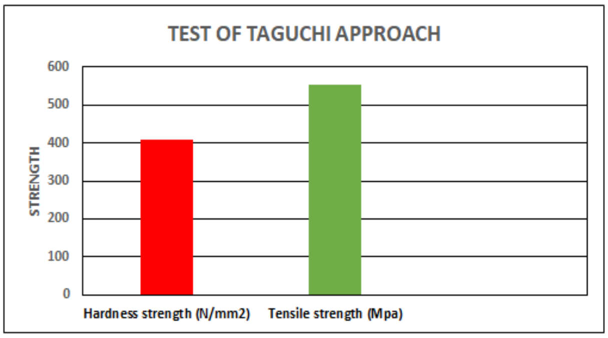

Figure-13. Test of Taguchi method.

Table-7. Result of validation tests of Taguchi's method.

S. No	Properties	Results
1.	Hardness strength N/mm^2	410
2.	Tensile strength (Mpa)	550

Table-7 specifies the result of validation test of Taguchi method, which denotes the hardness, tensile strength by the results of 410N/mm^2 and 550 Mpa as illusttrated in above table.

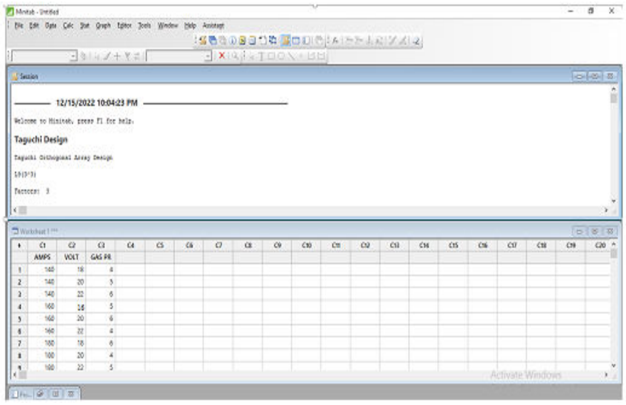

Figure-14. Create taguchi design in Minitab software.

A Taguchi Orthogonal array is first aimed using Minitab-17 to determine the S/N ratio. To Create the Taguchi Design, enter the variables in the Minitab as illustrated in Figure-14. A window for Taguchi design appears, after that click the shortcut on the desktop to launch the Minitab.

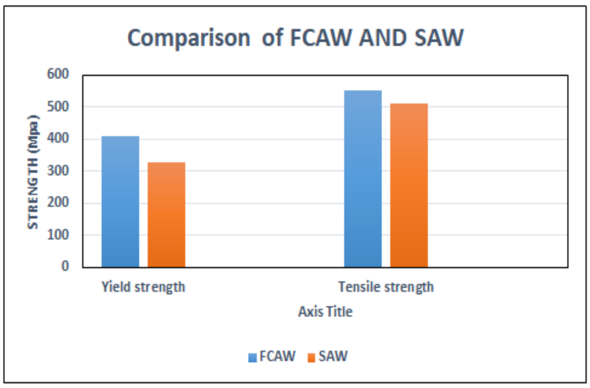

Figure-15. Comparison of FCAW and SAW.

The comparison graph for FCAW and SAW is illustrated in Figure-15, from the analyze it is clear that the proposed technique of FCAW achieves high yield strength and tensile strength when compared to the conventional method of SAW.

Table-8. Comparison of FCAW and SAW.

S. No	Properties	FCAW	SAW
1.	Yield strength	410	550
2.	Tensile strength	329	513

Table-8 illustrated the comparison of FCAW and SAW, the properties of yield and tensile strength are compared with the proposed technique of FCAW and the conventional method of SAW.

4. CONCLUSIONS

An investigation of the Flux Coir arc welding of EN8 and EN19 high-strength steel is conducted in this study. Each sample is prepared by varying the welding method parameters, such as the input voltage, current, wire feed, and speed. The quality of the weld is calculated by the yield strength, Microscopic analysis, and tensile strength. The high tensile strength of (570 MPa) and yield strength (493MPa) is achieved in sample 3, which are measured by using the predefined experiment with the parameters of voltage 21.12 v, current 172A, Wire feed rate is 5.9 m/min, welding speed is 75mm. The welding strength of sample 3 has increased with an input of average current. The microstructural analysis is made for 5 samples in FCAW, sample 3 and 5 give the best grain structure than the GMAW. Taguchi Orthogonal array is planned in minitab-17 to estimate the S/N ratio. As a result, the comparison graph obtained for FCAW and SAW, from that the proposed technique achieves higher tensile and yield strength than the conventional method.

REFERENCES

[1] Prabhu D., Jomy J. and Prabhu P. R. 2022. Influence of Different Heat Treatment Temperatures on the Microstructure and Corrosion Behaviour of Dual-Phase EN8 Steel in 0.5 M Sulphuric Acid Solution. Journal of Bio-and Tribo-Corrosion. 8(4): 88.

[2] Burger S., Zinke M. and Jüttner S. 2021. The hot cracking tendency of flux-cored arc welding with flux-cored wires of types Ni 6625. Welding in the World. 65: 381-392.

[3] Arifin A., Gunawan A. M., Yani I., Pratiwi D. K., Yanis M. and Sani K. A. 2019. Optimization of Angular Distortion on Weld Joints Using Taguchi Approach. Jurnal Kejuruteraan. 31(1): 19-23.

[4] Payares-Asprino C. 2021. Prediction of mechanical properties as a function of welding variables in robotic gas metal arc welding of duplex stainless steels SAF 2205 welds through artificial neural networks. Advances in Materials Science. 21(3): 75-90.

[5] Kim J., Kim J. and Pyo C. 2020. A study on fiber laser welding of high-manganese steel for cryogenic tanks. Processes. 8(12): 1536.

[6] Kuryntsev S. 2021. A review: Laser welding of dissimilar materials (Al/Fe, Al/Ti, Al/Cu)-Methods and techniques, microstructure and properties. Materials. 15(1): 122.

[7] Son H. J., Jeong Y. C., Seo B. W., Hong S. T., Kim Y. C. and Cho Y. T. 2023. Weld Quality Analysis of High-Hardness Armored Steel in Pulsed Gas Metal Arc Welding. Metals. 13(2): 303.

[8] Kamal S., Parthiban V., Puthilibai G., Thirumal Azhagan M., Kamal N., Senthil T.S. and Yishak S. 2022. Investigation on tensile behaviour of different weld joints through Taguchi approach. Advances in Materials Science and Engineering.

[9] Singh V. P., Patel S. K., Ranjan A. and Kuriachen B. 2020. Recent research progress in solid state friction-stir welding of aluminium-magnesium alloys: a critical review. Journal of Materials Research and Technology. 9(3): 6217-6256.

[10] Viyay P., SasiKumar V., Pannerselvam R., Soma Sundharam G. and Srinivasan N. An investigation on effect of process parameter on bi-metallic weld joints in fcaw with taguchi design. International Journal of Creative Research Thoughts (IJCRT). 9(3): 2320-2882.

[11] Li T., Zhang Y., Gao L. and Zhang Y. 2018. Optimization of FCAW parameters for ferrite content in 2205 DSS welds based on the taguchi design method. Advances in Materials Science and Engineering. 2018. pp. 1-7.

[12] Tavares S. S. M., Pardal J. M., Noris L. F. and Diniz M. G. 2021. Microstructural characterization and non-destructive testing and of welded joints of duplex stainless steel in flexible pipes. Journal of Materials Research and Technology. 15, pp. 3399-3408.

[13] Prabhu D., Jomy J. and Prabhu P. R. 2022. Influence of Different Heat Treatment Temperatures on the Microstructure and Corrosion Behaviour of Dual-Phase EN8 Steel in 0.5 M Sulphuric Acid

Solution. Journal of Bio-and Tribo-Corrosion. 8(4): 88.

[14] Roshan C. C., Raghul C., Ram H. V., Suraj K. P. and Solomon J. 2019. Non-destructive testing by liquid penetrant testing and ultrasonic testing-A review. Int. J. Adv. Res. Ideas Innov. Technol. 5, pp. 694-697.

[15] Park M., Kim J., Pyo C., Kim J. and Chun K. 2021. A Study on the Weldment Hardening Discrimination Procedure and Improvement of Flux Cored Arc Welding Process of ASTM A553-1 (9% Nickel Steel) Material Using Bead Geometry Distribution. Metals. 11(8): 1282.

[16] Zhao Y., Cao Y., Wen W., Lu Z., Zhang J., Liu Y. and Chen P. 2023. Effects of Mn content on austenite stability and mechanical properties of low Ni alumina-forming austenitic heat-resistant steel: a first-principles study. Scientific Reports. 13(1): 5769.

[17] Huang G., Wu J., Yuan R., Yang J., Cao F., Midawi, A.R., Guan W., Hou W., Lu C., Gerlich A. and Shen Y. 2022. Elucidating microstructural evolution and its effect on the mechanical properties of FSWed alumina-forming austenitic steel for power plant applications. Materials & Design. 215, pp. 110484.

[18] Prabhu P. R., Hiremath P., Prabhu D., Gowrishankar M. C. and Gurumurthy B. M. 2021. Chemical, electrochemical, thermodynamic and adsorption study of EN8 dual-phase steel with ferrite-martensite structure in 0.5 MH 2 SO 4 using pectin as inhibitor. Chemical Papers. 75, pp. 6083-6099.

[19] Ghosh N., Pal P. K., Nandi G. and Rudrapati R. 2018. Parametric optimization of gas metal arc welding process by PCA based Taguchi method on austenitic stainless steel AISI 316L. Materials Today: Proceedings. 5(1): 1620-1625.

[20] Mohammed S., Alkhaldi Ali A., Majeed Ali., Sobhi Khirallah. 2021. Impact of the Welding Parameters on the Width of the Welding beat in TIG Carbon Steel Welding. International Journal of Engineering and Advanced Technology (IJEAT). 10(3): 2249-8958.